Experimental Determination of Anisotropy Fields, First and Second Anisotropy Constants, and Remanent Magnetizations in Self-Polarized Zn–Ti and Co–Ti Equally Co-Substituted BaM Ferrites

Antoine Hoez, Jean-Luc Mattei, Alexis Chevalier

Experimental Determination of Anisotropy Fields, First and Second Anisotropy Constants, and Remanent Magnetizations in Self-Polarized Zn–Ti and Co–Ti Equally Co-Substituted BaM Ferrites

Antoine Hoez[1], Jean-Luc Mattei[1], Alexis Chevalier[1]

[1]Lab-STICC, UMR CNRS 6285, Université de Bretagne Occidentale, Brest, FRANCE

M-type hexagonal barium ferrites $Ba(M_xTi_x)Fe_{12-2x}O_{19}$ (M = Co or Zn, x = 0–0.5) were synthesized by chemical topotactical reaction. Both randomly oriented and self-polarized samples were prepared. Experimental values of the anisotropy fields, first and second anisotropy constants, and remanent magnetizations were extracted by combining hysteresis loops and microwave measurements. A salient result of this study is that, compared with K_1, K_2 cannot be disregarded for these co-doped BaM hexaferrites, even at low doping levels. Results show that the BaM ferrites of composition $Ba(Co_xTi_x)Fe_{12-2x}O_{19}$ are more suitable for microwave applications that operate at frequencies between 30 GHz and 40 GHz.

***Index Terms*— Co-substituted hexaferrites, Magnetocrystalline anisotropy, Remanent magnetization, Self-polarized hexaferrites**

I. Introduction

M-TYPE BARIUM hexaferrites (BaM) have long attracted attention for microwave and millimeter wave (MMW) applications [1], [2]. The interest of self-polarized BaM material properties is evident for the design of integrated and miniature MMW devices such as circulators, in which the external permanent magnet would be eliminated [3]. The modeling of MMW devices that use self-polarized materials requires, among other inputs, the values of the saturation magnetization M_S, remanent magnetization M_R, and magnetocrystalline anisotropy field H_K. For unsubstituted BaM, H_K = 1360 kA/m [4]. It was noted that lowering this value of H_K might be desirable for new MMW devices [5]. Iron substitution that could allow H_K lowering leads the easy axis of magnetization to become closer to the basal plane [4], this process being driven by the values of the anisotropy constants K_1 and K_2. The present paper reports a study of Co–Ti and Zn–Ti equiatomic co-substitution of M-type hexagonal barium ferrites $Ba(M_xTi_x)Fe_{12-2x}O_{19}$ (BaM-MTi, with M = Co or Zn, and x = 0–0.5) with two objectives. Firstly, to adjust anisotropy field H_K to meet different MMW application requirements (reduction in the value of H_K in order to lower the operating frequency, while maintaining a value of M_R/M_S close to 0.8), and secondly to determine the first (K_1) and second order (K_2) anisotropy constants for each of these compositions. To do this a law of approach to saturation (LAS), that was developed with the first and second order anisotropy constants K_1 and K_2, was used once the anisotropy field H_K had first been determined from microwave experiments. The presented method for the determination of K_1 and K_2 from magnetic experiments on polycrystalline material is new. The reduced remanent magnetization ($m_R = M_R/M_S$) is also reported. To the best of our knowledge, no previous published works have reported simultaneous studies of the variations of the anisotropy constants of H_K and of m_R on self-polarized BaM ferrites.

II. Preparation of Materials and Experimental Details

A. Synthesis of self-polarized and isotropic co-doped BaM materials

Chemical syntheses were made of two co-doped barium ferrites of composition $Ba(M_xTi_x)Fe_{12-2x}O_{19}$, where M represents Co or Zn, and with x = 0–0.5. Two sets of materials were prepared because of the different requirements in the experimental processes that were followed. The first set consisted in isotropic polycrystalline materials formed by randomly dispersed particles. Samples of this set are noted MTi-x-R, where R stands for random. The samples forming the second set are highly anisotropic, of the self-polarized type. Samples of this set are noted MTi-x-SP, where SP stands for self-polarized. They were prepared by controlled topotactic reaction [6]. The difference between the manufacturing of these two sets of materials lies exclusively in the nature, and consequently the geometric form, of the iron oxide that is used as a precursor: Hematite is used for the isotropic materials, goethite for the anisotropic materials. This is summarized in Table 1. Samples of both sets were of cylindrical shape (height 1.6 mm and diameter 6.8 mm). Details on the synthesis are as follows. Anisotropic polycrystalline samples of barium ferrites of BaM-MTi were fabricated from barium carbonate $BaCO_3$ (Acros Organics, Germany, 99%), titanium oxide TiO_2 (99.9%, Sigma-Aldrich), zinc oxide ZnO (99.9% Sigma-Aldrich), cobalt hydroxide $Co(OH)_2$ (99.9%, Sigma-Aldrich) and goethite FeO(OH) synthesized in the laboratory from iron III hexahydrate (Sigma-Aldrich, USA, 98%). The main key for a successful process in manufacturing BaM self-polarized materials is to use lath-shaped goethite crystallites, with a shape factor (thickness to length ratio) close to 0.15. For reasons of confidentiality, the process of goethite synthesis is not detailed. These components were carefully mixed using a manual mortar. The resulting mixtures were pressed into cylindrical pellets (7 mm in diameter and 5 mm thick) at a pressure of 320 MPa(uniaxial pressing). The direction of the applied pressure defines the c axis, perpendicular to the upper surface of the pellets. The pellets were then sintered at 1040°C, without steps. The goethite crystallites are in the form of laths, with a

crystallographic axis [001] oriented perpendicular to the largest face of the crystallite (Fig. 1a). The pressure applied during the molding step leads to a spontaneous preferential orientation of the goethite crystallites, with the [001] axes predominantly parallel to the direction of the applied pressure (Fig. 1c). Regarding the isotropic polycrystalline samples of BaM ferrites, the manufacturing process remained the same as for the anisotropic samples, as illustrated in Fig. 1c), except that spherical hematite crystallites were used, instead of goethite crystallites.

MTi-x-R materials were used for magnetic measurements (first magnetization curve, K_1 and K_2 values) and for microwave measurements (H_K values). MTi-x-SP were used to determinate M_R/M_S from hysteresis loops.

B. Expermimental details

X-ray diffraction analysis was carried out on a Panalytical Empyrean (Cu Kα radiation). Rietveld refinements revealed that the insertion of the dopants into the BaM crystal structure was effective to within about 10%. Magnetic measurements were performed using a Vibrating Sample Magnetometer EZ9 from MicroSense, with a maximum applied field intensity of 1500kA/m. The broadband complex permeability of each isotropic sample was measured in the frequency band 10 GHz–60 GHz by the transmission/reflection method using a Rohde and Schwarz ZVA67 vector network analyzer. The sample was placed on the top of a high-frequency microstrip line to measure the transmission (S21) and reflection (S11) parameters. For each composition, the values of H_K were measured using the MTi-x-R set of samples (Table 1). With this objective, the anisotropy fields H_K were deduced from the resonant frequency f_R determined by the maximum of the imaginary part μ" of the intrinsic permeability of the samples from the MTi-x-R set. Actually, the relationship between H_K and f_R is written as $f_R = \gamma H_K$, where γ is the gyromagnetic ratio ($\gamma = 35.12\ 10^{-3}$ MHz/A.m^{-1}).

TABLE I. FEATURES OF THE PRECURSORS AND TEXTURING OF THE OBTAINED BAM MATERIALS

Chemical precursors	Barium Carbonate	Hematite
Chemical formula	$BaCO_3$	Fe2O3
Shape	Spherical	Spherical
Texturing of $BaFe_{12}O_{19}$ material after pressing proceess	No texturing. Isotropic material. Random spatial distibution of the BaM particles (Figure 2c)	

Chemical precursors	Barium Carbonate	Goethite
Chemical formula	$BaCO_3$	FeO(OH)
Shape	Spherical	Lath
Texturing of $BaFe_{12}O_{19}$ material after pressing proceess	Texturing from BaM particles stacking. Anisotropic material (Figure 2c)	

The X-ray diffraction patterns of the goethite before and after the pressing process confirm the preferential orientation of the particles: the [101] direction, which is closest to [001] among those contributing to the diffraction pattern, is clearly the one that remains with high intensity.

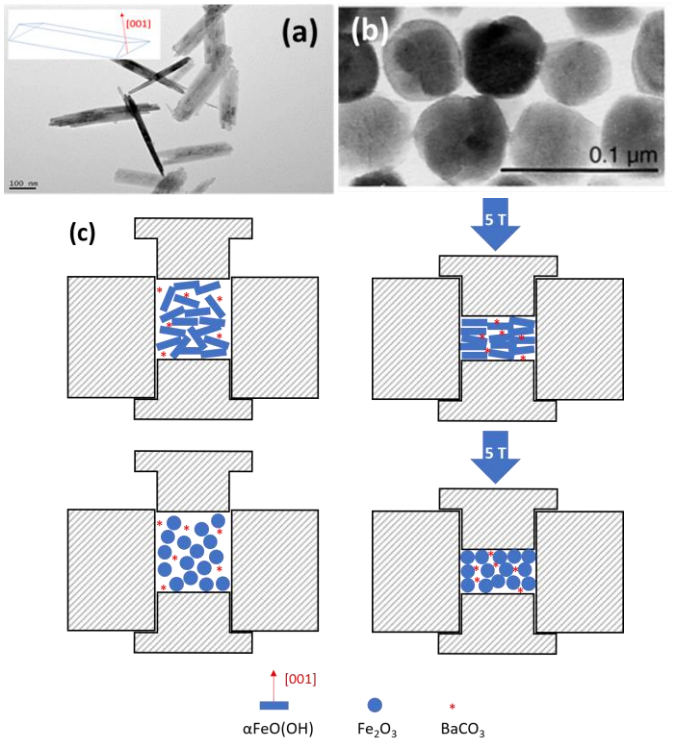

Fig. 1. TEM images of (a) lath-shaped goethite crystallites and (b) spherical hematite crystallites used for the manufacture of anisotropic and isotropic BaM ferrites, respectively; (c) Schematic representation of the powder compaction process. In this illustration, the mixture is constituted by barium carbonate spheres (red color) and, in blue color, either hematite (isotropic material, bottom) nor goethite laths (anisotropic material, top). The alignment in the basal plane of goethite crystallites is caused by the uniaxial pressure.

All other Bragg diffraction peaks that existed before compaction are extinguished (Figs. 2b and 2d). The SEM images show that the stacking of particles in the case of a sample made from goethite is clearly evident (Fig. 2c), in contrast with the random distribution of the particles elaborated from hematite (Fig. 2a).

Our objective was to determine the anisotropy constants K_1 and K_2 of each of the $Ba(M_xTi_x)Fe_{12-2x}O_{19}$ compositions. For this purpose, a saturation approach law (LAS) was used, together with the anisotropy field H_K value that had previously been determined from microwave experiments. MTi-x-R materials were used for the magnetic measurements (first magnetization curve, K_1 and K_2 values) and for the microwave measurements (H_K values). MTi-x-SP were solely used to determine M_R/M_S from their hysteresis loops.

III. MAGNETIC AND MICROWAVE MEASUREMENTS

For the study of remanent magnetization, hysteresis loops were measured on all MTi-x-R samples, in directions parallel and perpendicular to their basal plane.

These cycles are completely similar, with $m_R = 0.5$, demonstrating the isotropy of the materials. Whereas, on the whole MTi-x-SP samples, these hysteresis loops are significantly different, characteristic of anisotropic material (Fig. 3).

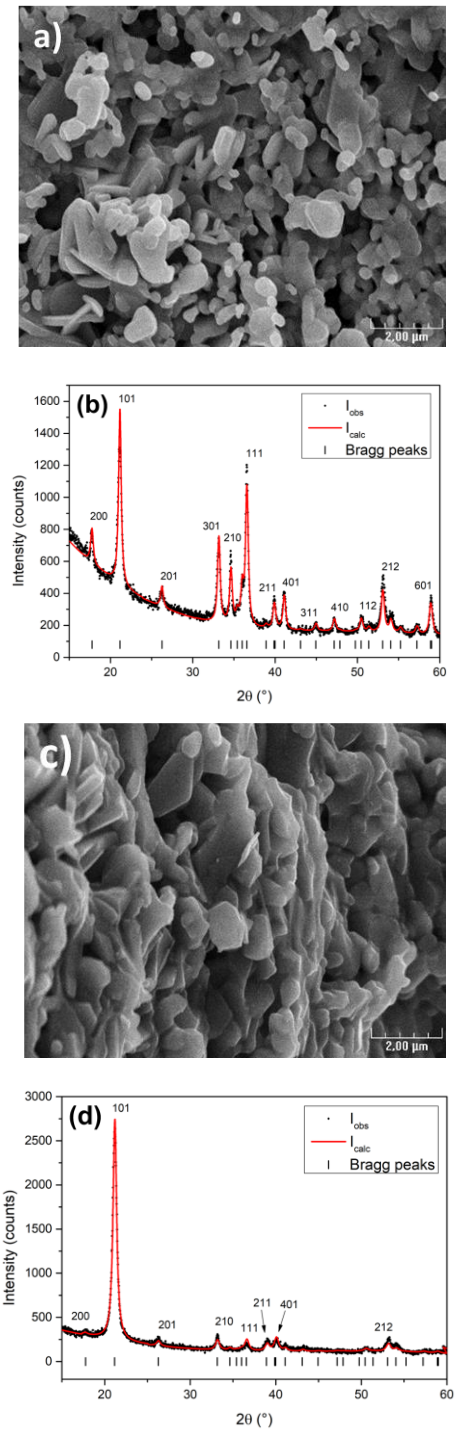

Fig. 2. SEM images of samples constituted either by randomly dispersed BaM particles (a) or oriented BaM particles (c). Rietveld analysis of goethite before (b) and after (d) the compaction process, respectively.

As an illustration, Fig. 4 shows the hysteresis cycles (in reduced magnetization) obtained from measurements in the $\vec{n}$ direction on the doped materials with x = 0.1, for the samples whose particles are either oriented or randomly dispersed. The fits of $M(1/H_i^2)$ in a strong field (H_i = 1340-1500 kA/m) are presented in Fig. 5, for x = 0, 0.1, 0.3, and 0.5, for $Ba(Co_xTi_x)Fe_{12-2x}O_{19}$. They concern the first magnetization curve measured on materials with a random distribution of particles. A linear variation of $M(1/H_i^2)$ is observed in this field range.

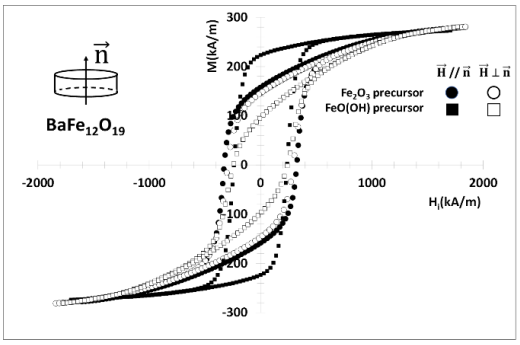

Fig. 3. Hysteresis cycles of the material $BaFe_{12}O_{19}$, prepared either from hematite or goethite as iron oxide precursor. The former (circles) is typical of isotropic material, with similar measured magnetizations along or perpendicular to $\vec{n}$, while the latter (squares) shows a behaviour characteristic of anisotropic material.

An illustration of the results obtained from measurements in the microwave range, allowing us to obtain the anisotropy field H_K values, is given in Fig. 6, where the frequency evolution of the isotropic material $BaFe_{12}O_{19}$ is shown. The anisotropy field H_K was deduced from the resonant frequency determined by the maximum of the imaginary part μ" of the intrinsic permeability, from the relationship $f_R = \gamma H_K$.

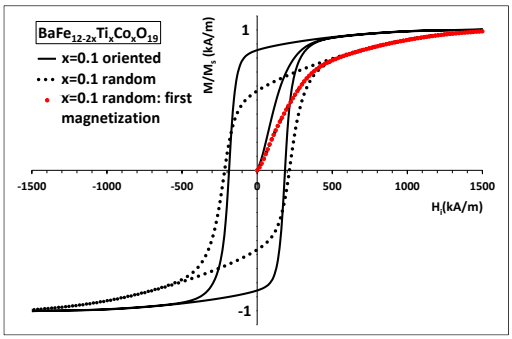

Fig. 4. Hysteresis cycles of the material $Ba(Co0.1Ti_{0.1})Fe_{11.8}O_{19}$, depending on whether it consists of randomly oriented particles (black dots) or stacked particles (solid line); the red dotted curve is the first magnetization curve.

The maximum of the imaginary μ''(f) occurs for f_R = 46.6 GHz, which corresponds to H_K = 1330 kA/m (i.e., 16.6 kOe). This result agrees with the value of the anisotropy field H_K of BaM ferrites, which is close to 1360 kA/m (i.e., 17 kOe). The values of H_K thus obtained for the doped hexaferrites are reported in Table II.

IV. K_1 AND K_2 DETERMINATION. DISCUSSION.

The law of approach to saturation (LAS), which is widely used for the analysis of the magnetization curves of polycrystalline magnetic materials, can be used to estimate the magnetic anisotropy field H_K. For a polycrystalline magnetic material consisting of randomly oriented crystallites, the magnetization M(H) tends towards its saturation value MS according to the empirical expression [7]–[9]:

$$M(H) = M_S(1-a/Hi -b/Hi^2)+\chi_p Hi \quad (1)$$

where $H_i = H_0 - H_d$, H_0 is the applied field and H_d is the demagnetizing field.

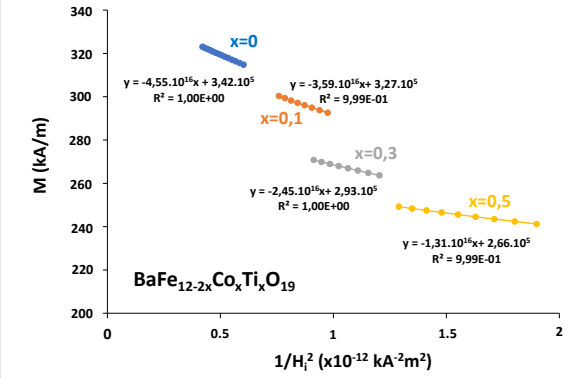

Fig. 5. $M(1/H_i^2)$ linear behavior, for some of the $Ba(Co_xTi_x)Fe_{12-2x}O_{19}$ compositions.

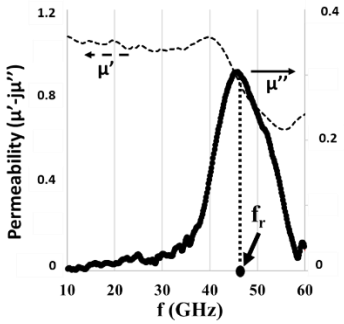

Fig. 6. Complex permeability spectra for an isotropic $BaFe_{12}O_{19}$ sample.

The term a/H, which results from the presence of inclusions and defects, must vanish at sufficiently high magnetic fields. The last term, χ_P , is a small high-field susceptibility, called the paraprocess. It is due to high-field band splitting and can be ignored below moderately applied field intensities [8]. The b/H^2 term arises from the reorientation of magnetic moments when the anisotropy axis is misaligned with the applied field. It is directly related to the magnetocrystalline anisotropy (even to H_K or to the first anisotropy constant K_1). Then, within a range of high enough internal fields, the following relation (2) is commonly used to derive M_S and the anisotropy field for an isotropic distribution of magnetic moments which can change direction only by rotating against the magnetic anisotropy [10]:

$$M(H) = M_S(1-b/H_i^2) \quad (2)$$

For uniaxial systems such as BaM particles, the expression for b is directly related to the magnetocrystalline anisotropy by $b = -H_K^2/15$ [10]. The calculation of the first order anisotropy constant K_1 is often done from here, then using the relation [11]:

$$H_K = (2K_1 + 4K_2)/(\mu_0 M_S) \quad (3)$$

In situations where $K_1 >> K_2$, this leads to $b = -4K_1^2/15$. However, this common assumption cannot be fulfilled for doped materials with x>0 because the condition $K_1 >> K_2$ might not be satisfied even at low doping values (although this is often assumed to be the case). On the one hand, both constants can be deduced from the Sucksmith–Thompson plot of H/M versus M^2, but this method was developed for single crystals and is not suitable for polycrystalline materials [12] as it leads to underestimated K_1 and overestimated K_2. It is, therefore, difficult to obtain the two anisotropy constants K_1 and K_2 of polycrystalline samples clearly. However, on the other hand, it can be shown that the LAS for randomly oriented crystallites with uniaxial anisotropy, and now considering the first and second anisotropy constants, can be written (where $M(H_i)$ is the component of the magnetization along the field H_i):

$$M(H_i) = M_S\left(1 - \frac{4}{315}\frac{21K_1^2+48K_1K_2+32K_2^2}{(\mu_0^2 M_S^2)}\right)\frac{1}{H_1^2} \quad (4)$$

Details of this calculation are given in Appendix A. From the measured first magnetization curves, the linear variation of M vs. $1/H_i^2$ was observed for all samples in the appropriate field range, after correction for the demagnetizing field. The determination coefficients R^2 in M vs. $1/H_i^2$ linear relations are in any case better than 0.999 (Fig. 5).

The variations of K_1 and K_2 as functions of x were determined from the measurements of H_K using microwave experiments and its relationship with K_1 and K_2 (1), on one hand, and from the slope of straight line $M(H_i)$ against $1/H_i^2$ (2), on the other. $K_1(x)$ and $K_2(x)$ are shown fig.7.

A previous study reported on comparable, although lower, K_1 and K_2 values for a co-doped $BaFe_{11.2}Co_{0.4}Ti_{0.4}O_{19}$ single crystal [13]: $1.033x10^5$ J/m^3 and $K_2 = 0.08x10^5$ J/m^3 . The values of the constants K_1 and K_2 presented in [13] were obtained using the Sucksmith and Tompson method, dedicated to single crystals. The method we use is suitable for polycrystalline materials, and does not have the limitations of Sucksmith and Tompson's method [14]. We therefore believe that the values we present are reliable. It is clear that, compared with K_1, K_2 cannot be disregarded for co-doped (Co–Ti) and (Zn–Ti) BaM hexaferrites, even at low doping levels. The data in Table 1 show that both M_R/M_S and H_K decrease with increasing doping for the $Ba(M_xTi_x)Fe_{12-2x}O_{19}$ self-polarized samples. However, the decrease of H_K is more rapid, and that of M_R/M_S slower, for $Ba(Co_xTi_x)Fe_{12-2x}O_{19}$ than for $Ba(Zn_xTi_x)Fe_{12-2x}O_{19}$. In particular, $Ba(Co_xTi_x)Fe_{12-2x}O_{19}$ with x = 0.3 shows quite a high $M_R/M_S = 0.77$ value, together with H_K = 11.6 kOe, which corresponds to the resonance frequency f_R = 32.5 GHz. These features make barium hexaferrites of composition $Ba(Co_xTi_x)Fe_{12-2x}O_{19}$ more suitable for MMW applications.

TABLE II. REMANENT MAGNETIZATIONS AND ANISOTROPY FIELDS

	M_R/M_S		H_k (kA/m)	
x	(ZnTi)x	(CoTi)x	(ZnTi)x	(CoTi)x
0	0.92	0.92	1336	1336
0.1	0.84	0.86	1224	1288
0.2	0.77	0.82	1112	1208
0.3	0.73	0.80	1048	1088
0.4	0.72	0.77	968	928
0.5	0.70	0.75	888	824

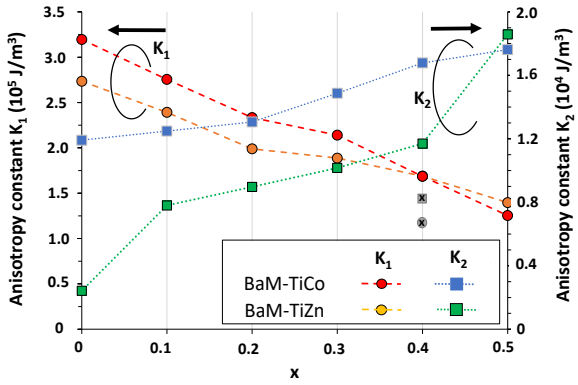

Fig. 7. First and second order anisotropy constants plotted against the doping level x. Symbols in grey are data are extracted from [13].

APPENDIX A

We consider the magnetization of a ferromagnet in a narrow region around ferromagnetic saturation approaches to saturation via rotation process with a small angle between the magnetization and the applied field (Fig. A1).

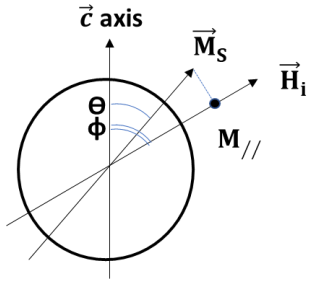

Fig. A1 . Spherical particle with uniaxial magnetocrystalline anisotropy.

For a single-crystal particle of BaM, with uniaxial anisotropy, the magnetocrystalline energy variation for a saturation approach is written, at order 2: $W_K=K_1\sin^2\Theta+K_2\sin^4\Theta-\mu_0 M_s\cos(\phi-\Theta)+1/2\mu_0 N_d M_S^2$, where ϕ and Θ are the angles that the internal field $\vec{H}_i$ and the magnetization $\vec{M}_S$ make with the easy axis, respectively, N_d being the shape anisotropy factor. The equilibrium position of the magnetization is deduced from the condition $dW/d\Theta=0$. Assuming moreover that in strong fields the condition $\phi-\Theta \to 0$ is verified, one easily obtain: $M_{//} = M_S\left(1-{}^1/_{(\mu_0^2 M_S^2)}\cdot{}^1/_{H_i^2}\cdot(2K_1^2\sin^2\phi\cos^2\phi + 4K_1K_2\sin^4\phi\cos^2\phi + 8K_2^2\sin^6\phi\cos^2\phi\right)$. Then, in the case of a BaM polycrystal, where the axes of easy magnetization are randomly distributed, the component $<M_{//}>$ of the magnetization along the field H_i results from an average taken over the different orientations of the c axis writes: $< M_{//} >= M_S\left(1-{}^1/_{(\mu_0^2 M_S^2)}\cdot{}^1/_{H_i^2}\cdot(2K_1^2 < \sin^2\phi\cos^2\phi > +4K_1K_2 < \sin^4\phi\cos^2\phi > +8K_2^2 < \sin^6\phi\cos^2\phi >)\right)$, where the brackets indicate an average value made on the sphere of unit radius. We thus obtain: $< M_{//} >= M_S\left(1-{}^1/_{(\mu_0^2 M_S^2)}\cdot{}^1/_{H_i^2}\cdot{}^4/_{315}\cdot(21K_1^2 + 48K_1K_2 + 32K_2^2)\right)$.

ACKNOWLEDGMENT

This work is partially supported by a public grant overseen by the French National Research Agency (ANR-20-ASTR-0010, CONTACT project).

REFERENCES

[1] V. G. Harris *et al.*, "Recent advances in processing and applications of microwave ferrites," *J. Magn. Magn. Mater.*, vol. 321, no. 14, pp. 2035–2047, 2009, doi: 10.1016/j.jmmm.2009.01.004.

[2] A. Geiler, A. Daigle, J. Wang, Y. Chen, C. Vittoria, and V. Harris, "Consequences of magnetic anisotropy in realizing practical microwave hexaferrite devices," *J. Magn. Magn. Mater.*, vol. 324, no. 21, pp. 3393–3397, 2012, doi: 10.1016/j.jmmm.2012.02.050.

[3] T. Sakai, Y. Chen, C. N. Chinnasamy, C. Vittoria, and V. G. Harris, "Textured Sc-Doped Barium – Ferrite Compacts for Microwave Applications Below 20 GHz," *October*, vol. 42, no. 10, pp. 3353–3355, 2006.

[4] R. C. Pullar, "Hexagonal ferrites: A review of the synthesis, properties and applications of hexaferrite ceramics," *Prog. Mater. Sci.*, vol. 57, no. 7, pp. 1191–1334, 2012, doi: 10.1016/j.pmatsci.2012.04.001.

[5] Q. Li, Y. Chen, C. Yu, L. Young, J. Spector, and V. G. Harris, "Emerging magnetodielectric materials for 5G communications: 18H hexaferrites," *Acta Mater.*, vol. 231, p. 117854, 2022, doi: 10.1016/j.actamat.2022.117854.

[6] A. Hoez, J. Mattei, and A. Chevalier, "New Manufacturing Process for Granular Texture Management in Polycrystalline BaM Hexaferrites Through the Goethite Crystallite Laths Aspect Ratio, and a Specialized Law of Ap-proach to the Magnetic Saturation for Partly Polarized Uniaxial Materials," *Magnetochemistry*, vol. 9, no. 30, 2023.

[7] S. Chikazumi, *Physics of magnetism*. Stanley H. Charap, 1978.

[8] J. M. D. Coey, *Magnetism and magnetic materials*. 2010.

[9] Z. W. Li, L. Chen, C. K. Ong, and Z. Yang, "Static and dynamic magnetic properties of Co2Z barium ferrite nanoparticle composites," *J. Mater. Sci.*, vol. 40, no. 3, pp. 719–723, 2005, doi: 10.1007/s10853-005-6312-y.

[10] J. Herbst and F. Pinkerton, "Law of approach to saturation for polycrystalline ferromagnets: Remanent initial state," *Phys. Rev. B - Condens. Matter Mater. Phys.*, vol. 57, no. 17, pp. 10733–10739, 1998, doi: 10.1103/PhysRevB.57.10733.

[11] W. Sucksmith and J. E. Thompson, "The magnetic anisotropy of cobalt," *Proc. R. Soc. London, Ser. A*, vol. 225, p. 362, 1954.

[12] K. Y. Ho, X. Y. Xiong, J. Zhi, and L. Z. Cheng, "Measurement of effective magnetic anisotropy of nanocrystalline Fe-Cu-Nb-Si-B soft magnetic alloys," *J. Appl. Phys.*, vol. 74, no. 11, pp. 6788–6790, 1993, doi: 10.1063/1.355078.

[13] J. P. Kreisel; Vincent, H.; Tasset, F.; Paté M. and Ganne;, "An investigation of the magnetic anisotropy

change in BaFe12-2xTixCoxO19 single crystals," *J. Magn. Magn. Mater.*, vol. 24, pp. 17–29, 2001.

[14] A. S. Bolyachkin, D. S. Neznakhin, and M. I. Bartashevich, "The effect of magnetization anisotropy and paramagnetic susceptibility on the magnetization process," *J. Appl. Phys.*, vol. 118, no. 21, 2015, doi: 10.1063/1.4936604.